

Evaluation of the Fukushima Daiichi Unit 4 Spent Fuel Pool

Bruce R. Hugo¹, Ronald P. Omberg²

¹Energy Northwest, USA

²Washington State University, USA;

Corresponding author: BRHugo@frontier.com

Received: 06 May 2015; accepted: 04 August 2015

Abstract

Accurate prediction of evaporative losses from spent nuclear storage pools (SFPs) is important for activities ranging from sizing of water makeup systems during plant design to predicting the time available to supply emergency makeup water following severe accidents. A new evaporation model based on diffusion has been proposed that makes substantially different predictions compared with other correlations for evaporation under conditions of high water temperature and forced air flow. Analysis of the Fukushima Daiichi Unit 4 SFP response to a prolonged loss of cooling has provided the only high temperature evaporation data with forced air flow present. The diffusion based evaporation model is compared with two other modern evaporation correlations.

Keywords

Spent Fuel Storage; Evaporation; Fukushima Daiichi Accident

1.0 Introduction

1.1 Applications of Evaporation Modelling

An accurate model of evaporation is desirable for a number of applications related to spent nuclear storage pool (SFP) design, operation, maintenance, and accident response. Following a severe event such as the prolonged loss of electrical power that occurred during the 2011 Fukushima Daiichi accident, neither cooling nor normal makeup to the SFP may be available. When emergency makeup capability is available, there will be competing needs for reactor pressure vessel (RPV) injection for core cooling, containment injection for containment cooling, and SFP makeup to maintain the spent fuel covered with water. An accurate method of determining cumulative evaporation losses from the SFP is essential for deciding when to shift emergency makeup from the RPV or containment to the SFP. Premature diversion of water to the SFP could result in unnecessary additional damage to the core or containment; late makeup could result in damage to spent fuel and significant additional releases of radioactivity.

1.2 The Diffusion Model of Evaporation

An evaporation correlation was proposed in reference [1] that uses the solution to Fick's equation for unimolar diffusion and boundary layer theory as its mathematical basis. This "diffusion correlation" has the form:

$$E = 9.24 \left(1 + 2\nu^{1.35} \right)^{0.67} \frac{T}{273K} \ln \frac{P - \phi P_{\text{sat},a}}{P - P_{\text{sat},w}} \quad (1)$$

Eq. (1) applies for uniform air flow of velocity ν over the water surface. For a SFP, this type of forced air flow would only be present following damage to the SFP building that results in exposure of the water surface to wind. When the SFP building is intact and air is drawn over the water surface from the ventilation system (e.g., by exhaust ducts in one or more sides of the SFP) then the velocity term is replaced by a SFP-specific correction factor:

$$E = 11.6 \frac{T}{273K} \ln \frac{P - \phi P_{\text{sat},a}}{P - P_{\text{sat},w}} \quad (2)$$

1.3 The Shah Correlation

Shah [2] has proposed the following correlation for evaporation when air velocity is at least 0.15 m/sec:

$$E = 0.00005 \left(\frac{\nu}{0.15} \right)^{0.7} (P_{\text{sat},w} - \phi P_{\text{sat},a}) \quad (3)$$

Shah uses the analogy between heat and mass transfer under natural convection conditions to obtain:

$$E = 35\rho_w(\rho_a - \rho_w)^{1/3}(\omega_w - \omega_a) \quad (4a)$$

$$E = 0.00005(P_{\text{sat},w} - \phi P_{\text{sat},a}) \quad (4b)$$

Shah recommends that the larger result of Eq. (4a) and (4b) be used when air velocity is less than 0.15 m/sec.

Shah's correlation and the diffusion correlation provide similar evaporation rate predictions for forced air flow with low water temperatures and for water temperatures up to 90°C with stagnant air. Before the Fukushima Daiichi accident, there were no published evaporation data for high water temperatures with forced air flow. Data recently available from the Fukushima Daiichi Unit 4 SFP allow a comparison of the Shah and diffusion correlations for the combination of high water temperature and forced air flow conditions.

2.0 The Fukushima Daiichi Unit 4 SFP

2.1 Background

The March 2011 earthquake and tsunami that disabled all offsite and onsite power at the four unit Fukushima Daiichi nuclear power plant resulted in significant core damage to three of its Boiling Water Reactors (BWRs). The fourth BWR had no fuel in its reactor vessel during the accident as a full core offload to the Unit 4 SFP had been performed to support refueling outage maintenance. As a result, the Unit 4 SFP had a significantly higher than normal decay heat load and there was considerable concern that the loss of water due to evaporation could result in the recently irradiated fuel becoming uncovered and overheated. Due to building damage, loss of normal electrical power, and high radiation fields, it was not initially possible to measure the SFP levels directly. With only limited emergency water makeup equipment available, cooling water was diverted from reactor core and containment cooling to make up for the unknown losses from the Unit 4 SFP.

2.2 Accident Sequence

The Unit 4 SFP lost normal cooling on March 11 with an initial water temperature of about 27°C and a decay heat load of 2.28 MW [3]. A hydrogen explosion damaged the Unit 4 SFP building on March 15, exposing the SFP water surface to the weather. Water level in the SFP dropped due to evaporation until makeup water additions began on March 20 and were continued intermittently [3].

The day before the hydrogen explosion the Unit 4 SFP temperature was measured at 84°C. The next

temperature measurement was not obtained until April 12 when the SFP had reached 90°C; radioactive decay had by then reduced the decay heat loading to 1.98 MW. Thereafter most of the water temperature readings were between 82°C and 90°C.

3.0 Analysis Methodology

3.1 Non-Evaporative Ambient Losses

Non-evaporative ambient losses consist of heat conduction through the SFP floor and walls, radiation heat transfer from the water surface to the environment, and convective heating of the air at the water surface. An initial calculation was performed that included use of a one-dimensional transient conduction model for the heat losses through the walls, along with natural convection and (after the reactor building was damaged) forced convection heat losses to the air above the SFP. A quasi-equilibrium SFP wall temperature distribution was attained after a few days after which the total non-evaporative heat losses were approximately proportional to the temperature difference between the SFP water and the outdoor air temperature. Non-evaporative ambient losses were found to be 8-12% of the total ambient heat losses from the pool.

3.2 Evaporative Losses

After the Unit 4 SFP building was damaged, evaporation from the SFP water surface was influenced by wind driven air flow through the building. Fukushima area meteorological data are available for the associated dates from [4], but the air flow across the water surface would have been less than the outside air speed due to two factors: the resistance to air flow provided by the remaining portions of the building structure, and the large vertical distance between the water surface and the top of the SFP. The Shah and diffusion correlations were both developed using published data for which the distance from the pool edge to the water surface is a much smaller fraction of the pool width.

Since the actual air flow across the SFP water surface cannot be calculated, an alternate approach was used to evaluate the Shah and diffusion correlations. The evaporative heat losses were found by subtracting the estimated non-evaporative heat losses from the known decay heat input. The air velocity required to produce the evaporative heat loss was then found using each correlation.

The forced air flow evaporation predictions provided by the Shah and diffusion correlations diverge appreciably at water temperatures above 27°C. A small part of this departure is the different functional form for the effect

of air flow: the Shah correlation uses a $v^{0.7}$ term while the diffusion correlation's velocity term is approximately proportional to $v^{0.9}$ for air velocities above 1 m/sec.

The largest difference between the Shah and diffusion correlations for forced air flow is the functional dependence on water temperature. As illustrated in Fig. 1, the evaporation rate predictions (Eq. (1) and Eq. (4a)) for cold stagnant air are similar for the two correlations. Shah's Eq. (4b) rises much more slowly with water temperature but this has no impact on the stagnant air prediction since the Shah approach uses the larger of Eq. (4a) and (4b). Eq. (4b) dominates only when the density of the moist air at the water surface is lower than that of the dry air above (the water must be significantly cooler than the air).

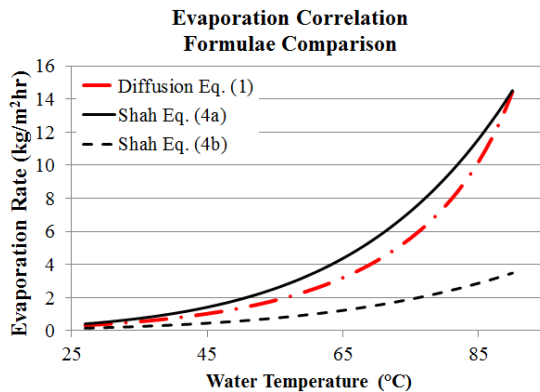


Fig. 1 Correlation Formulae Comparison

But for forced air flow (above 0.15 m/sec), the Shah correlation uses Eq. (3) which is equivalent to Eq. (4b) multiplied by an air velocity correction term. Thus for forced air flow, the diffusion correlation Eq. (1) and the Shah correlation Eq. (3) will provide significantly different evaporation rate predictions.

3.3 Other Assumptions

The Unit 4 SFP wall outer surfaces were assumed to be exposed to outside air temperature following the loss of the reactor building ventilation system. No air flow over the SFP surface was assumed from the time of the loss of AC power until the hydrogen explosion. Following the hydrogen explosion, a fixed ratio between the outdoor wind speed and the air velocity across the water surface was assumed; this ratio was varied to reproduce the SFP temperature data reported in [3].

Historical Fukushima weather data [4] were used. Average wind speed and relative humidity data were used for each day. Minimum temperature was assumed to occur at 4 a.m. and maximum temperature at 4 p.m. with linear variation between these points.

The water makeup rate and SFP level data from reference [4] were used to adjust calculated SFP water mass.

4.0 Results

4.1 Diffusion Correlation

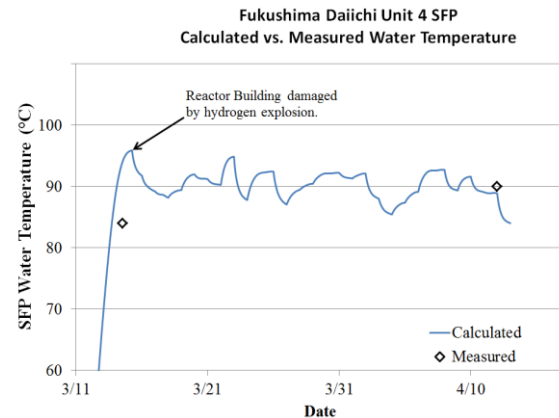


Fig. 2 SFP Calculated and Measured Temperature

Fig. 2 shows the calculated Unit 4 SFP water temperature for the month following the accident. Only two water temperature measurements are available for this period. The first temperature measurement of 84°C on March 14 was taken while the SFP was still heating up to an equilibrium condition; this explains why a relatively low temperature (compared with later measurements) was observed during a period when the decay heat loading was near its maximum for the period.

Once the reactor building was open to the atmosphere, wind driven air flow over the SFP surface had a significant impact on the equilibrium water temperature. A water surface air velocity of 20% of outside wind speed was found to provide good agreement with the April 12 water temperature measurement of 90°C.

Subsequent water temperature measurements were mostly in the 82°C to 90°C range. The diffusion correlation predicts (based on the decay heat loading and estimate of non-evaporative ambient losses) water surface air velocities of 1.5 m/sec and 0.6 m/sec respectively for these water temperatures.

The thermal time constant (time required for SFP water temperature to reach 63.2% of its ultimate temperature change following a step change in the heat removal rate) of the SFP system was found to be 9.5 hours, so the SFP temperature is mostly determined by the average wind speed during the previous 12 hours.

Table 1 compares the SFP surface air velocity required to produce the observed SFP temperature data from [3] with the average wind speed from [4]. The diffusion correlation predicts the observed SFP temperatures if

the air velocity at the SFP surface is 21% of the outside wind speed. This appears to be a reasonable ratio given the obstructing effect of the intact portions of the reactor building and the lowered SFP water level. Based on [3], the SFP water level was up to 4 meters below the top edge of the SFP during the period 4/12 to 5/7.

One entry in Table 1 appears to be an outlier: the 69.4°C measurement on 4/28 but this was during a period when the SFP had been nearly refilled to its normal level. The ratio of surface air velocity to wind speed would be much closer to 100% with the SFP water level near the upper edge. The water level was one meter lower by the time the next measurement was taken.

Table 1: Calculated SFP Air Velocities Using the Diffusion Correlation

Date (2011)	T_{SFP} (°C)	Air Velocity Required (m/sec)	Average Wind Speed (m/sec)	Fraction
4/12	90.0	0.58	6.3	9%
4/22	90.6	0.49	1.3	37%
4/23	82.6	1.37	5.4	26%
4/24	85.3	1.02	4.9	21%
4/25	80.0	1.67	3.6	47%
4/26	84.4	1.10	2.7	41%
4/27	80.9	1.57	4.0	39%
4/28	69.4	3.66	4.9	74%
4/29	91.6	0.35	3.6	10%
4/30	91.6	0.35	3.1	11%
5/1	91.6	0.36	4.9	7%
5/2	91.6	0.34	4.5	8%
5/3	91.6	0.34	2.2	15%
5/4	90.1	0.48	2.7	18%
5/5	92.6	0.22	3.1	7%
5/6	87.9	0.68	2.7	25%
5/7	85.6	0.92	4.9	19%
Average				21%

4.2 The Shah Correlation

When the analysis described in section 4.1 is repeated using the Shah correlation, higher calculated SFP surface air velocities are required to reproduce the observed SFP temperature measurements. As shown in Table 2, for some data the recorded wind speed is not high enough to produce the observed SFP temperatures even with no air flow attenuation.

Table 2: Calculated SFP Air Velocities Using the Shah Correlation

Date (2011)	T_{SFP} (°C)	Air Velocity Required (m/sec)	Average Wind Speed (m/sec)	Fraction
4/12	90.0	2.17	6.3	35%
4/22	90.6	2.02	1.3	150%
4/23	82.6	3.18	5.4	59%
4/24	85.3	2.69	4.9	55%

4/25	80.0	3.62	3.6	101%
4/26	84.4	2.79	2.7	104%
4/27	80.9	3.49	4.0	87%
4/28	69.4	6.89	4.9	140%
4/29	91.6	1.82	3.6	51%
4/30	91.6	1.82	3.1	58%
5/1	91.6	1.83	4.9	37%
5/2	91.6	1.80	4.5	40%
5/3	91.6	1.80	2.2	81%
5/4	90.1	1.95	2.7	73%
5/5	92.6	1.67	3.1	53%
5/6	87.9	2.16	2.7	80%
5/7	85.6	2.47	4.9	50%
Average				74%

4.3 The Wang et al. Evaporation Model

Wang et al. in reference [3] proposed an evaporation model based on an analogy between the heat transfer and mass transfer rate for free convection at the SFP surface. Although the Shah free convection correlations (Eq. (4a) and (4b)) are also based on a heat transfer analogy, the Wang model has a different functional form and makes significantly higher evaporation rate predictions above 75°C as illustrated in Fig. 3.

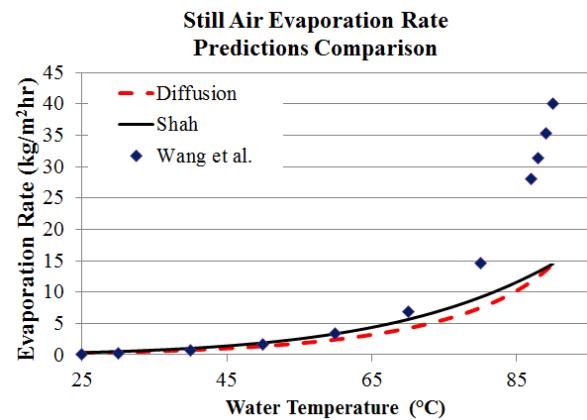


Fig. 3 Still Air Evaporation rate Predictions Comparison

Wang et al. conclude that that removal of decay heat from the Unit 4 SFP can be entirely attributed to evaporation and that the effect of forced air flow on the evaporation rate is negligible. These conclusions are questionable. The other ambient heat losses, while smaller than those due to evaporation, account for about 10-12% of the decay heat input. Additionally, the SFP temperature would remain fairly constant if water temperature was the only significant variable affecting the evaporation rate. Instead, a significant number of SFP temperature measurements were below the 90°C required to remove the ~2 MW produced by decay heat.

5.0 Conclusions

Although there is a lot of data scatter, the diffusion correlation provides a relatively good prediction of the observed Unit 4 SFP temperature measurements if the air velocity at the water surface is assumed to be 20% of the wind speed whenever the SFP water level is at least one meter below the top edge of the SFP.

The Shah correlation requires an air flow rate equal to 75% of the wind speed to reproduce the Unit 4 SFP temperature data. This appears to be unrealistic due to the obstructing effect of the remaining portions of the reactor building structure and the water surface being several meters below the SFP edge when most of the water temperature data were taken.

Any evaporation model that does not include the effects of forced air flow, which was present to some degree following the hydrogen explosion, cannot account for the observed variations ($>8^{\circ}\text{C}$) of SFP temperature with time.

6.0 Nomenclature

E	evaporation rate, $\text{kg/m}^2\text{hr}$
$P_{\text{sat},w}$	saturation pressure of water at pool water temperature, Pa
$P_{\text{sat},a}$	saturation pressure of water at ambient air temperature, Pa
T	Temperature, K
v	air velocity, m/sec
ϕ	relative humidity, dimensionless

7.0 References

1. Hugo, B. R. et al. Predicting Evaporation Rates From Spent Nuclear Fuel Storage Pools. International Nuclear Safety Journal. 2014; 3; 1:50-56.
2. Shah, M. M. Methods for Calculation of Evaporation from Swimming Pools and Other Water Surfaces. ASHRAE Transactions. 2014;120(2); 3-17.
3. Wang, D. et al. Study of Fukushima Daiichi Nuclear Power Station Unit 4 Spent-Fuel Pool. Nuclear Technology. 2012;(180); 205-215.
4. Weather Underground. 2015. Available from: www.wunderground.com